RESEARCH ARTICLE

Ecologically Friendly Biofunctional Ink for Reconstruction of Rigid Living Systems Under Wet Conditions

Alan Avila-Ramírez[1], Alexander U. Valle-Pérez[1], Hepi Hari Susapto[1], Rosario Pérez-Pedroza[1], Giuseppina R. Briola[1], Abdulelah Alrashoudi[1], Zainab Khan[1], Panayiotis Bilalis[1], Charlotte A. E. Hauser[1,2]*

[1]Laboratory for Nanomedicine, Division of Biological and Environmental Science and Engineering, King Abdullah University of Science and Technology, Thuwal 23955-6900, Saudi Arabia
[2]Computational Bioscience Research Center (CBRC), King Abdullah University of Science and Technology, Thuwal 23955-69900, Saudi Arabia

Abstract: The development of three-dimensional (3D)-printable inks is essential for several applications, from industrial manufacturing to novel applications for biomedical engineering. Remarkably, biomaterials for tissue engineering applications can be expanded to other new horizons; for instance, restoration of rigid living systems as coral reefs is an emergent need derived from recent issues from climate change. The coral reefs have been endangered, which can be observed in the increasing bleaching around the world. Very few studies report eco-friendly inks for matter since most conventional approaches require synthetic polymer, which at some point could be a pollutant depending on the material. Therefore, there is an unmet need for cost-effective formulations from eco-friendly materials for 3D manufacturing to develop carbonate-based inks for coral reef restoration. Our value proposition derives from technologies developed for regenerative medicine, commonly applied for human tissues like bone and cartilage. In our case, we created a novel biomaterial formulation from biopolymers such as gelatin methacrylate, poly (ethylene glycol diacrylate), alginate, and gelatin as scaffold and binder for the calcium carbonate and hydroxyapatite bioceramics needed to mimic the structure of rigid structures. This project presents evidence from 2D/3D manufacturing, chemical, mechanical, and biological characterization, which supports the hypothesis of its utility to aid in the fight to counteract the coral bleaching that affects all the marine ecosystem, primarily when this is supported by solid research in biomaterials science used for living systems, it can extend tissue engineering into new approaches in different domains such as environmental or marine sciences.

Keywords: Bioprinting; Biopolymers; Bioceramics; Rigid tissue; Crosslinking; Ecofriendly

*Correspondence to: Charlotte A. E. Hauser, Laboratory for Nanomedicine, Division of Biological and Environmental Science and Engineering, King Abdullah University of Science and Technology, Thuwal 23955-6900, Saudi Arabia; charlotte.hauser@kaust.edu.sa

Received: June 15, 2021; **Accepted:** July 21, 2021; **Published Online:** August 19, 2021

Citation: Avila-Ramírez A, Valle-Perez AU, Susapto HH, *et al.,* 2021, Ecologically Friendly Biofunctional Ink for Reconstruction of Rigid Living Systems Under Wet Conditions. *Int J Bioprint*, 7(4):398. http://doi.org/10.18063/ijb.v7i4.398

1. Introduction

Biomaterials have been essential elements in developing technologies that counteract the current issues in the biomedical field[1]. On the other hand, there is a strong interest from the industry to create new technologies based on eco-friendly biopolymers that can be cost-effective for the current needs in the market[2]. Therefore, several studies coming from the development of biomaterials are a trending topic for medical applications. Researchers commonly look for natural sources that could potentially be chemically and physically modified to surpass their ground state behavior[3]. A couple of examples are gelatin and alginate as one of the classic materials for tissue regeneration. Gelatin comes from inexpensive natural sources; on the other side, alginate has ionic-crosslinking behavior that permits crosslinking with cations such as calcium. Both biopolymers are used for cartilage

replacements, bone regeneration, drug delivery, and even exciting uses for molecular gastronomy. Gelatin usually works as a viscous platform to bind other elements of interest.

Nevertheless, to expand the functionality of these materials in tissue engineering, the methacrylation reaction has been studied; in this case, the functionalization of gelatin can be photo-crosslinked by different wavelengths, depending on the photoinitiator (PI) used. This physicochemical improvement has permitted the usage of novel biofrabrication techniques[4]. Besides applications in wound dressings and hard tissues, cartilages or bones have been implemented with gelatin methacrylate (GelMA), with reinforcements with bioceramics as hydroxyapatite and other sort of inorganic particles[5,6]. In addition, poly (ethylene glycol diacrylate) (PEGDA) has been widely implemented due to its fast end effective crosslinking behavior, which can work as a complement to other photo-cross-linkable polymers[7].

Innovation should not be stuck in just a particular direction; conversely, there are other biological issues that our world is currently facing. Therefore, it is crucial to take action to adopt eco-friendly applications that could counteract problems derived from climate change. Thus, we aim to expand tissue engineering applications into a broader range of goals in this project. For instance, one of the most significant burdens from the environmental and marine sciences is coral bleaching, that in other words can be considered the disruption of a symbiosis that consists of a robust and rigid system of calcium carbonate with the living beings, which are mainly species of polyps derived from heat wave and changes in the marine ecosystem that bleaches the colonies and have strong effects in the marine biota[8,9]. For this reason, many groups around the world has started to take an interest in creating and developing new formulations and taking advantage of new innovative materials to counteract environmental problems as a way of preventing more extensive problems that will jeopardize the lives of human beings in the future[10,11]. Therefore, in this project, biopolymers as gelatin, alginate, gelatin methacrylate (GelMA), and poly (ethylene glycol diacrylate) (PEGDA) are reinforced with bioceramics as calcium carbonate and hydroxyapatite. This unique formulation can assist the growth of hard-living systems, like corals, as an innovative technology that ionic/photo-crosslink, which makes it adaptable to new 3D manufacturing technologies and can withstand under wet conditions (**Figure 1**).

2. Materials and methods

The following materials and reactants are necessary for obtaining the biopolymer base and bioceramics to develop the final paste and subsequently realize the fundamental characterization. The final formulation is homogenized into two main parts. The initial one is the biopolymer base that works as a binder and crosslinking material. The second is the bioceramics side that will reinforce the paste and mimic the paste hard-living structure, a standard coral. The materials used include GelMA (synthesized), gelatin from porcine skin (Sigma-Aldrich), alginic acid (Merck), PEGDA (Sigma-Aldrich), lithium phenyl-2,4,6 trimethyl-benzoyl phosphinate (Sigma-Aldrich), milli-Q water, hydroxyapatite (Sigma-Aldrich), calcium carbonate (Sigma Aldrich), dimethyl sulfoxide (DMSO) (Sigma-Aldrich), Dialyzer Maxi, molecular weight cut off (MWCO) 12 – 14 kDa (Merck), 0.22 μm bottle top vacuum filter (Corning), DMSO for Nuclear Magnetic Resonance (NMR) (Sigma-Aldrich), phosphate-buffered saline (PBS), pH 7.4 (Sigma-Aldrich), and syringe pump (Harvard Apparatus).

2.1. High GelMA (H-GelMA) synthesis

For a high degree of methacrylation of GelMA (**Figure S1**), that is, 10 g of gelatin, 100 mL 1 × PBS (sterile) was added. The mixture was dissolved with the aid of a heating plate (~240 rpm at 50°C). 8 mL of methacrylic anhydride was added dropwise with the assistance of a syringe pump and let emulsion rotate (240 rpm) at 50°C for 2 h. 100 mL of sterile PBS (50°C) was preheated to dilute GelMA solution for 10 min at 50°C. The dialysis membrane (MWCO 12-14,000 kDa) was prepared at 40°C, and GelMA solution was inserted inside them; dialysis was allowed to go on for a minimum of 5 days with constant stirring. The water was changed from 1 to 2 times a day to eliminate the excess methacrylate ions and dispose of the residue in a regulated container. A sterile vacuum (0.22 μm) filtration cup was used to filter the liquid. Sterilized polymer was transferred into Falcon tubes. Semi-closed tubes were submerged in liquid nitrogen and freeze-dried for at least 5 days to get a sponge-like freeze-dried GelMA sample[12].

2.2. Biopolymer-base preparation

Depending on the volume required to prepare and the percentages stated in **Table 1**, freeze-dried H-GelMA, gelatin, alginate, and PEGDA were dissolved in Milli-Q with constant stirring to dissolve the final solution. Using a heath bath is recommended to melt the solution at a temperature of the maximum of 50°C. A higher temperature can modify the molecular behavior of the four polymer chains and jeopardize the accuracy of printability. Then, the PI was added (Lithium phenyl-2,4,6 trimethylbenzoylphosphinate) to the previous solution. To avoid the interaction with light that triggers crosslinking reaction, it is recommended to cover it with aluminum foil. This base can be kept at −20°C for more extended periods if there is no interaction with light that could trigger gelation.

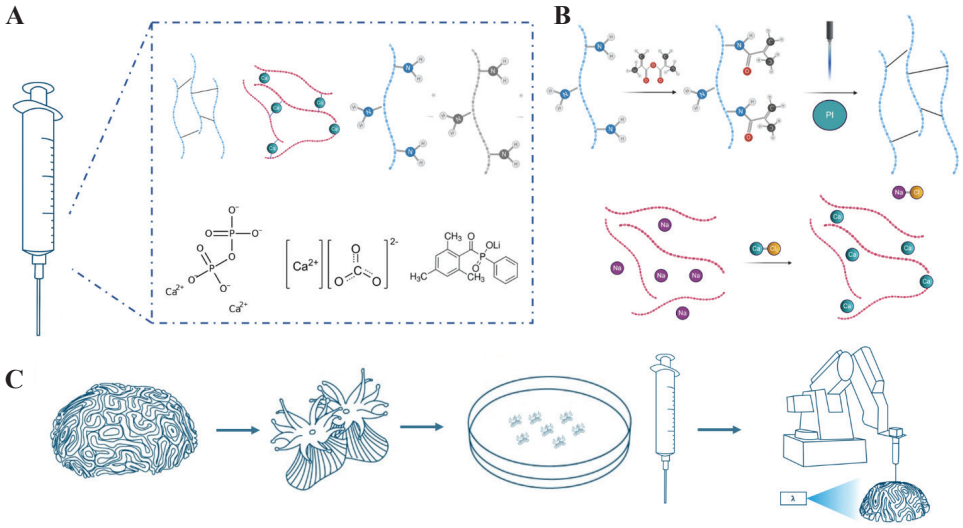

Figure 1. Explanation from the project's scope. (A) Integration of biopolymers gelatin, alginate, gelatin methacrylate, poly (ethylene glycol diacrylate), and bioceramics calcium carbonate and hydroxyapatite for potential rigid-living systems. (B) Schematics from the two primary sources of crosslinking to enhance printability, ionic-crosslinking with cations such as calcium and photo-crosslinking with a wavelength range from 365 nm to 405 nm. (C) The proposal for a potential future application with this material for rigid-living systems can be manufactured with extrusion-based 3D printing technologies.

Table 1. Formulation from the complete ink.

Biopolymer base	**Percentage W/W**	**Weight by cartridge sample**	**Purpose**
High gelatin methacrylate (H-GelMA)	2.50%	0.25 g.	Photo-crosslinking and printability
Poly (ethylene glycol diacrylate) (PEGDA) 700 MW	2.50%	0.25 g. ≈ 0.25 mL	Increase speed rate of photo-crosslinking
Alginic acid (Alg) Low MW	2.50%	0.25 g	Ionic-crosslinking with calcium
Gelatin (Gel)	2.50%	0.25 g	Viscosity for pre-crosslinked paste
Lithium phenyl-2,4,6 trimethylbenzoylphosphinate (LAP)	0.15%	0.015g	Photoinitiation 365(UV) – 405 (blue) nm
Bioceramics	**Percentage W/W**	**Weight in 10 mL.**	**Purpose**
Hydroxyapatite (HA)	40%	4 g	Density for under wet conditions
Calcium carbonate (CaCO3)	40%	4 g	Mimic coral chemical Structure
Solvent	**Quantity**	**Quantity**	**Purpose**
Milli-Q water	10 mL	10 mL	Dissolve

2.3. Bioceramics reinforcement

The quantity of bioceramics needed for the formulation is presented in **Table 1,** imbued at the biopolymer-based solution prepared previously. Solid and constant stirring with a thin spatula is crucial as the final homogenous product will be viscous, similar to a commercial bone paste. It is recommended to start 3D printing protocols with the fresh material to avoid premature crosslinking with the light or natural desiccation of water. The formulation is intended to be cost-effective because the biopolymer part from the formulation was designed at minimal concentrations without compromising its crosslinking properties and printing fidelity, relying on inexpensive materials for commercial 3D manufacturing technologies.

2.4. Manufacturing

Two methodologies were used for 3D manufacturing. The first one was molding of a flexible resin; it is designed in different designs derived from real branched and brain corals obtained in the red sea. The second one is 3D printing based on the implementation of two systems: A pressure-based bioprinter Inkredible from the Cellink company and the designed 6-°-of-freedom robotic arm system developed for bioprinting applications at our research group[13].

2.5. Image processing for 3D printing

The similarity structural index measurement (SSIM) was measured by comparing pixels between images (**Figure S2**); it can be visually seen how the comparison is made between two fixed figures to get this numerical value[14]. The response surface methodology (RSM) was applied to evaluate the effect of enhancing the developed ink with hydroxyapatite and calcium carbonate over the structural similarity index from the printed structure. According to the statistical modeling reported in recent studies[15,16], the elaboration of the RSM was performed with the MATLAB® software, and the model's constants were obtained with the Minitab 18 software (Minitab® LLC, USA). The general model is presented in **Equation 1**, and the simplified resulting model is shown in **Equation 2**.

$$\gamma = \delta_0 \pm \delta_1\alpha \pm \delta_2\beta \pm \delta_3\alpha^2 \pm \delta_4\beta^2 \pm \delta_5(\alpha\beta) + \varepsilon_{ijk} \quad (1)$$

Equation 1. A general model for the effect of hydroxyapatite and calcium carbonate over the structural similarity index of the printed structure; where Y is the response and α,β are the factors of the model, $\delta_{0,1,2,3,4,5}$ represent the constants of the model, and ε_{ijk} is the total error.

$$\gamma = \delta_0 + \delta_1\alpha - \delta_2\beta - \delta_3\alpha^2 + \delta_4\beta^2 \; ; \; \frac{\partial\gamma}{\partial i} = \varphi_i \quad (2)$$

Equation 2. A simplified model for the effect of hydroxyapatite and calcium carbonate over the structural similarity index of the printed structure; where Y is the response and α,β are the factors of the model, $\delta_{0,1,2,3,4}$ the constants of the model, i represents any of the two factors, and ϕ_i the solved values from the partial derivatives.

2.6. Morphological imaging

The scanning electron microscope FEI Magellan extreme-high-resolution imaging was applied to a grid of the 3D printed formulation, crosslinked, and dried overnight, with an accelerating voltage of 3 kV. The dried peptides were sputter-coated with 5 nm Ir before imaging. An optical microscope was used to obtain the macrography with a source of light in the upper side from the sample.

2.7. Chemical characterization

For Fourier-transform infrared (FTIR) spectroscopy, a Thermo Nicolet iS10 FTIR Spectrometer (Thermofisher) was used; the samples were prepared and crosslinked by two different sources individually compared to control with exposure at room conditions. For Solid-State NMR, the 13C Magic Angle Spinning (MAS) NMR spectra were recorded using Bruker Avance 400 MHz spectrometer (Bruker, USA) at room temperature. The sample was lyophilized. Bruker Topspin 3.5pl7 software (Bruker BioSpin, Rheinstetten, Germany) and MestReNova (Mestrelab Research, Spain) were used for data collection and analysis. In addition, Solution-State NMR, the NMR spectra (1H and 13C) of biopolymer-base were recorded using Bruker Avance 400 MHz spectrometer (Bruker, USA) at room temperature. The sample was prepared to dissolve 5 mg powder in 500 µl of d6-DMSO (Cambridge Isotope Laboratories, USA) and then transferred into 5 mm NMR tubes. Bruker Topspin 3.5pl7 and MestReNova software were used for data collection and processing, respectively, of NMR of H-NMR, C-NMR for the solid and liquid state, the PI was not added as it behaves similar to paramagnetic species; therefore, the equipment will not detect any significant signal. A complete sample of a printed coral was ground for X-ray diffraction compared with bioceramics spectra. For thermochemical characterization, both thermogravimetric analysis (TGA) and differential scanning calorimetry (DSC) (TA Instruments), the final printed inks were ground and analyzed by both instruments. Around 20 mg of material were used for each sample. The ranges of temperatures used, were 25-850°C for TGA and 25-400°C for DSC.

2.8. Viscoelastic characterization

The mechanical properties of non-crosslinked ink were analyzed using TA Ares-G2 Rheometer equipped with Advanced Peltier System. A freshly prepared ink was measured using an 8 mm parallel plate with a 1.8 mm gap at 25°C. The stiffness was analyzed through a time-sweep test for 5 min with angular frequency and one rad/s and 0.1% strain, respectively. A temperature sweep was subsequently performed on the sample by applying a gradual temperature increase from 25°C to 50°C with similar angular frequency and strain.

The viscosity of the ink before crosslinking was determined using 25 mm parallel plate geometry with a 0.5 mm gap at 25°C. Three replicate samples were measured using a 25 mm parallel plate geometry with a gap of 0.5 mm at 25°C. The flow experiment was set up by starting the shear rate from 0.001 to 300 s^{-1} for a 600-s duration. The value of the shear rate that we choose for our printing system was calculated using the equation below[17,18]:

$$\gamma = \frac{8Q}{\pi d^3} \quad (3)$$

Equation 3. γ: shear rate (s^{-1}); Q: flow rate (2 µL/s); d: diameter of needle (0.84 mm).

2.9. Biological assessments

Undifferentiated mesenchymal stem cells (MSCs) were seeded at a density of 15.5E3 cells/cm^2 and incubated for 7 days (5% CO_2, 37°C) in supplemented DMEM-F12

medium. The media were changed on the 4th day. Then, the treated cells were cultivated together with a droplet of 10 µL of crosslinked bioink. As a blank, a droplet was incubated in the same conditions, with no cells. As a control, cells were cultured without a droplet of bioink. The cells proliferation was measured using Alamar Blue (Invitrogen, CAT: DAL1025) by adding 1/10th of the volume directly to the cells, followed by 2 h of incubation. Fluorescence was read in a PheraStar plate reader (Ex/Em: 485/520). The cell viability was evaluated using the Live/Dead assay (Invitrogen, CAT: L3224).

3. Results and discussion

The ink was printed in an extrusion-based 3D printing at a pre-crosslinked state with the aid of the robotic arm system. In this example, several layers can be printed one over another without collapsing. Moreover, with the aid of blue light, crosslinking can aid in printing to invent more complex structures. For this case, we demonstrated that it could be done even at the ground state behavior from the formulation. For instance, with the incidence of blue light, the printed structure can be easier to manufacture and is more stable in the air or under wet conditions. An underwater printing test was done; a 2D structure of a grid and another at undersea water of the KAUST (**Figure 2C**) was printed and kept after 12 weeks in seawater. The printed structure did not have visible degradation and was derived from the photo-crosslinking of PEGDA and GelMA and ionic-crosslinking of alginate with calcium ions found in the filtered water obtained from the Red Sea, permitting the appliance of this material directly in damaged coral reefs.

In addition, as printing takes significant amounts of time, we established a 3D molding protocol. The ink was directly poured into the negative molds obtained from natural coral structures, where these samples were dried at room temperature overnight. These structures coming from the mold were rigid and complex. Consequently, this is a cost-effective methodology that does not require robust equipment.

During the formulation development, we noticed that the ink was enhanced by adding hydroxyapatite (to improve the under-water stability property) and calcium carbonate (to increase the stiffness from the

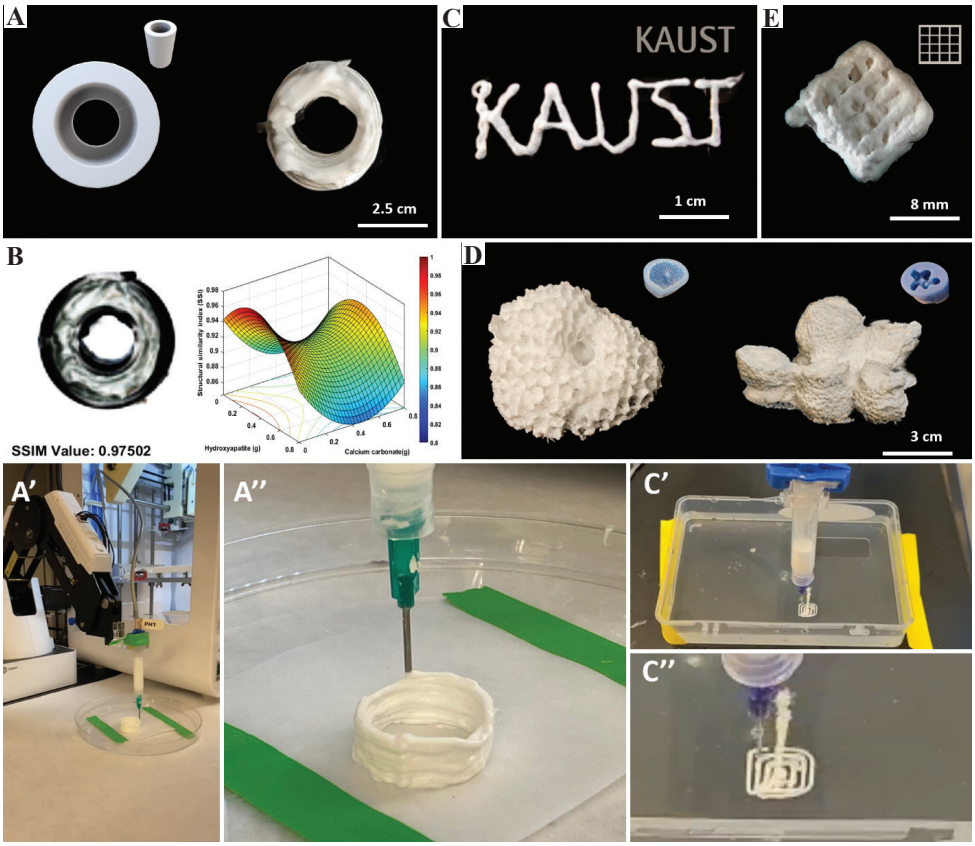

Figure 2. 2D/3D fabrication. (A-A") 3D printing of a 50-layer cylindric structure with the aid of an assembled 6-degree-of-freedom robotic arm system coupled with an extrusion-based bioprinter. (B) The image processing technique that is used to obtain a SSIM. (C-C") Manufacturing under wet conditions of structure KAUST one-layer structure and a squared-grid. (D) Molded structures dried at room temperature overnight. (E) Squared grid printed and details at millimetric scale after crosslinking and desiccation. Videos from A and C are included in the supplementary file.

printed or molded objects). It was observed that the integration of these two components to the original ink composition affected the overall structural definition of the printed objects (**Figure 2**). The contour plot representation of the surface response graph can be found as part of the supplementary material (**Figures S3 and S4**). The original ink exhibited a structural definition between 0.92 and 0.94; however, it was found that the definition could be improved (SSIM >0.95) by the addition of 0.1 g/cm^3 – 0.6 g/cm^3 of hydroxyapatite (**Figure 2**). On the other hand, the addition of calcium carbonate resulted in a lower structural definition (Soil-structure interaction [SSI] <0.92). Nevertheless, it was found that when adding both: calcium carbonate and hydroxyapatite, the structural definition from the printed object could be preserved (SSIM >0.92), even with the presence of the calcium carbonate in ink, possible when simultaneously adding 0.1 g/cm^3 – 0.2 g/cm^3 of calcium carbonate and 0.1 g/cm^3 – 0.6 g/cm^3 of hydroxyapatite (**Figure 2**). Similarly, the addition of 0.8 g/cm^3 ^{g} of calcium carbonate and 0.2 g/cm^3 – 0.6 g/cm^3 of hydroxyapatite resulted in a high structure definition. It is essential to highlight that adding beyond 0.7 g/cm^3 of hydroxyapatite in the presence of calcium carbonate reduces the structure definition (SSI <0.875) of the printed object (**Figure S3 and S4**). Therefore, the development of enhanced inks for under seawater printing without losing their printing definition can be carried by adding these two components to the original ink according to the previously described maximization conditions.

It is essential to clarify that due to the loss of solvent derived from room temperature desiccation, the structure was slightly deformed; however, as the solvent corresponds to a minimal portion compared to the rest of the constituents. For this reason, a fast image processing test was done, arrowing 97.5% similarity between a 3D printed cylinder of 50 layers after crosslinking and desiccation (**Figure 2B**). This analysis is an innovative way to characterize printing fidelity. Nevertheless, more improvements in the technique could be made in further studies to get more accurate results.

This ink was designed to a helpful a carrier for biological cargo in different orders of magnitude, depending on the biological species of interest that could go from 50 mm (corroborated at **Figure 7**) until the printing resolution of the assembled 3D printing system that experimentally was 1 mm (**Figure 3)**. In the scanning electron microscope images (**Figure 3B**), the binding from the polymer can be an attachment from the calcium carbonate and hydroxyapatite round crystals; GelMA and gelatin offer the porous platform to get the crystals incrusted due to its long polymer chains at a molecular level[19-21].

FT-IR corroborated the two crosslinking behaviors from the ink **(Figure 4A**); one clear result from the ionic-crosslinking comes from the OH peak observed at 3300 cm^{-1}, that states the covalent bonding between hydroxyl groups in alginic acid polysaccharides. The photo-crosslinked material and the exposure at room conditions are similar because the photoinitiation with a wavelength in the spectrum related to blue light can come from regular exposure to light; therefore, crosslinking occurs at a lower rate. Evidence from this is the peaks from N-H and C-H at 2950 cm^{-1} and 2990 cm^{-1}. Finally, carbonate

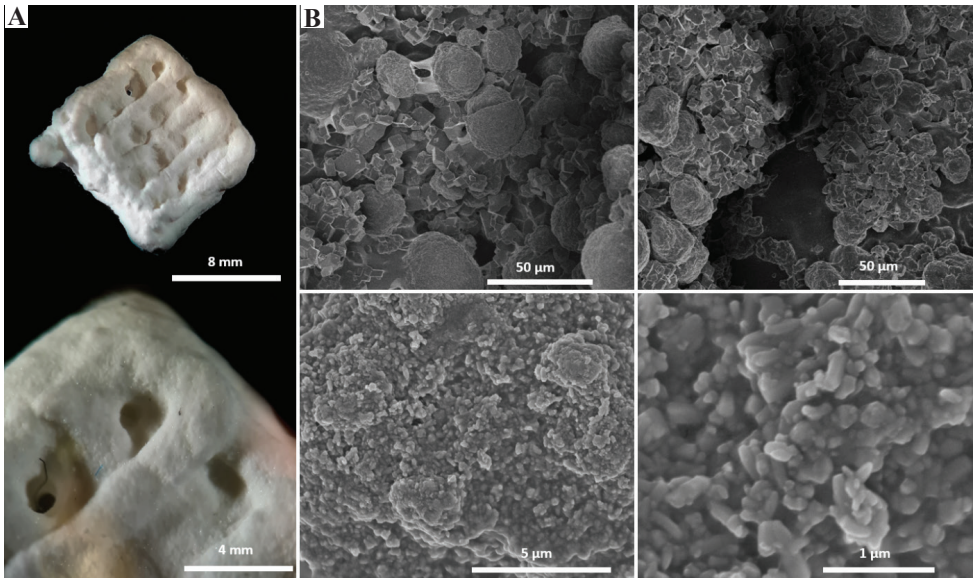

Figure 3. Morphological studies of a 3D dried printed grid. (A) Demonstration of the feasibility of printing at a resolution of approximately 1 mm, with the aid of a commercial extrusion-based bioprinter. (B) Scanning electron microscope (SEM) image of the same grid at the microscale at different sizes. To see the morphology of the surface and the binding from the bioceramics crystals to the polymer.

and phosphate ions appear in the 1400 cm^{-1} and 1000 cm^{-1} peaks, referring to bioceramics in the sample.

The peaks from XRD (**Figure 4B)** represent the mixture of bioceramics components from the ink. This study helped us understand ceramics' chemical interaction with the natural base polymer to corroborate its crosslinking behavior and binding with the polymer base[22,23]. Therefore, in the final formulation analysis, both calcium carbonate and hydroxyapatite peaks remained unaltered compared to the crystals from both bioceramics components, stating no crystal rearrangement or direct modification contact with the polymer source. Besides, the calcium carbonate peaks at 23°, 29°, 36°, 39°, 43°, 47°, 48°, and 58° correspond to a crystal structure reported in the literature as calcite, remarkably seen at the strong peak from 29°[24]. On the other side, hydroxyapatite's most representative signals appear at 26°, 32°, 39°, and 49° highlighting the intensity of the ones in between 30 and 35 that usually appears stronger according to the literature, and both of them can be observed in the supplementary measurements (**Figure S5)** where XRD was done just to each independent bioceramics[25].

The biopolymer structure was investigated using ^{13}C solid-state NMR spectroscopy. The differences between ^{13}C MAS NMR spectra (**Figure 4C)** of the sample without and with bioceramics can be distinguished. The most significant result is the double peak (blue box) appears between 155 and 135 ppm, which correspond to C=CH that result of the interaction of a C group from the polymer attached to carbonate ions from the sample[26].

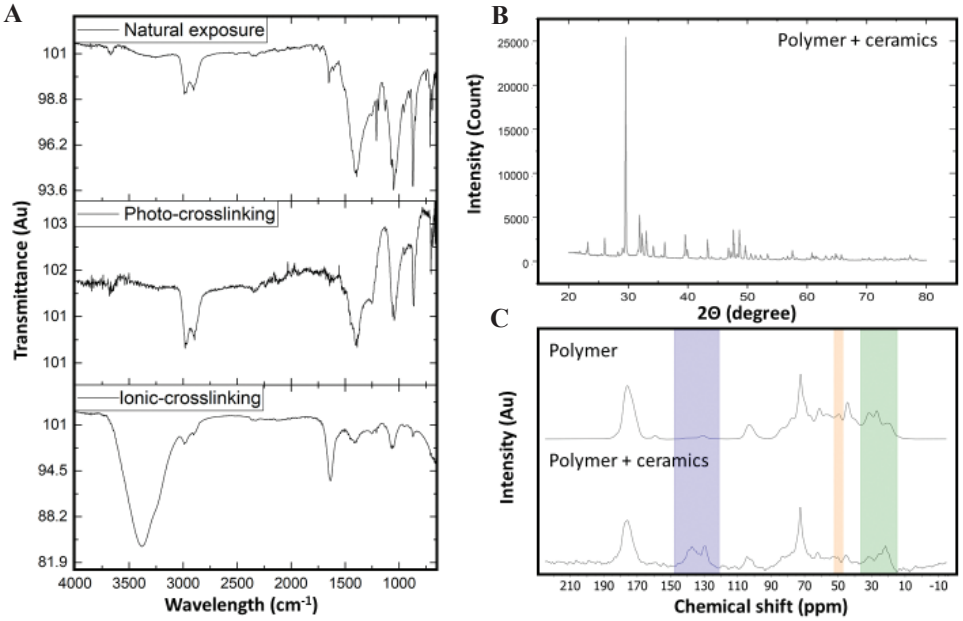

Figure 4. (A) Fourier-transform infrared spectra from the formulation under different crosslinking conditions, initially in room temperature conditions, with the incidence of blue-light at 405 nm and ionic-crosslinking with calcium chloride at 6% solution. (B) XRD-P spectra from ink formulation of the biopolymers and bioceramics. (C) ^{13}C magic angle spinning nuclear magnetic resonance spectra of biopolymers without (above) and with (below) bioceramics.

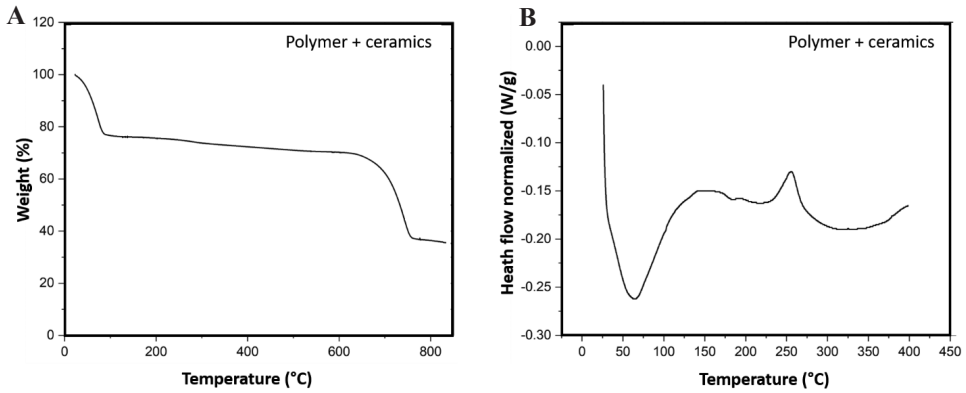

Figure 5. Thermal Analysis. (A) TGA and (B) DSC thermograms of bioceramics incorporated in the biopolymer base.

The rise in the orange box, at 50 ppm, and the green box, between 35 and 25 ppm, disappears when there are bioceramics; therefore, these signals are a piece of evidence from the interaction of binding from inorganic components of calcium, phosphate, and carbonate ions to the biopolymer side from the formulation. This data can be corroborated in future studies with ^{31}P MAS NMR and ^{43}Ca MAS NMR[27,28]. Besides, in ^{1}H-NMR (**Figure S6**), it can be complemented the presence of the methacrylation functionalization of the GelMA synthesis and PEGDA integration as the methacrylate ions can be observed between 6 and 6.5 ppm[28,29].

In the TGA (**Figure 5A**), there is a reduction of 13% of weight from 90°C to 100°C due to the loss of H_2O-coordinated ions remaining in the crystalline arrangements of ceramics compressed with the polymer. From 100°C to 642°C, there is a loss of 10% from the sample, equivalent to the biopolymers that were calcined under this procedure; this variation comes from the different polymeric ionic/photo-crosslinking behaviors

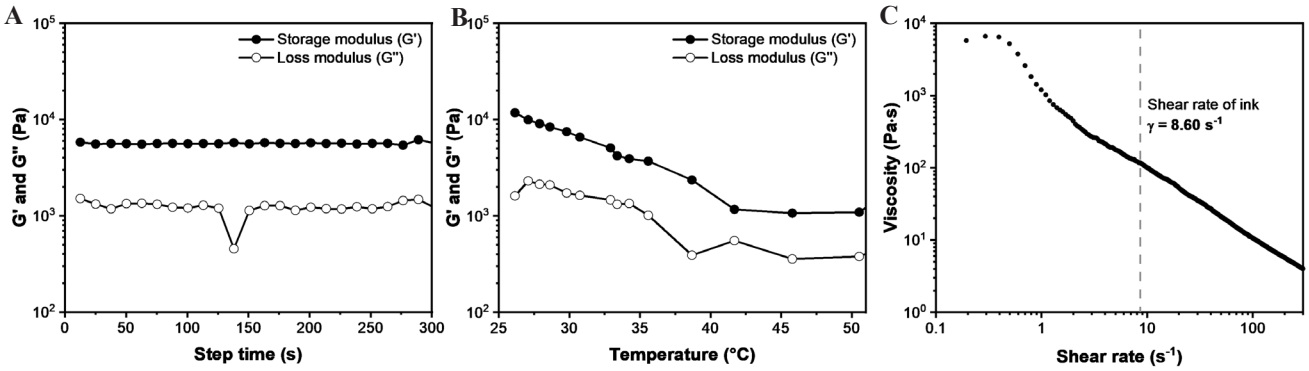

Figure 6. Rheological characterization of non-crosslinked ink. (A) Storage modulus (G') and loss modulus (G'') were measured for 5 min at 1 rad/s angular frequency, 0.1% strain, and 25°C. (B) Temperature sweep test at 1 rad/s and 0.1% strain. (C) Viscosity at different shear rates.

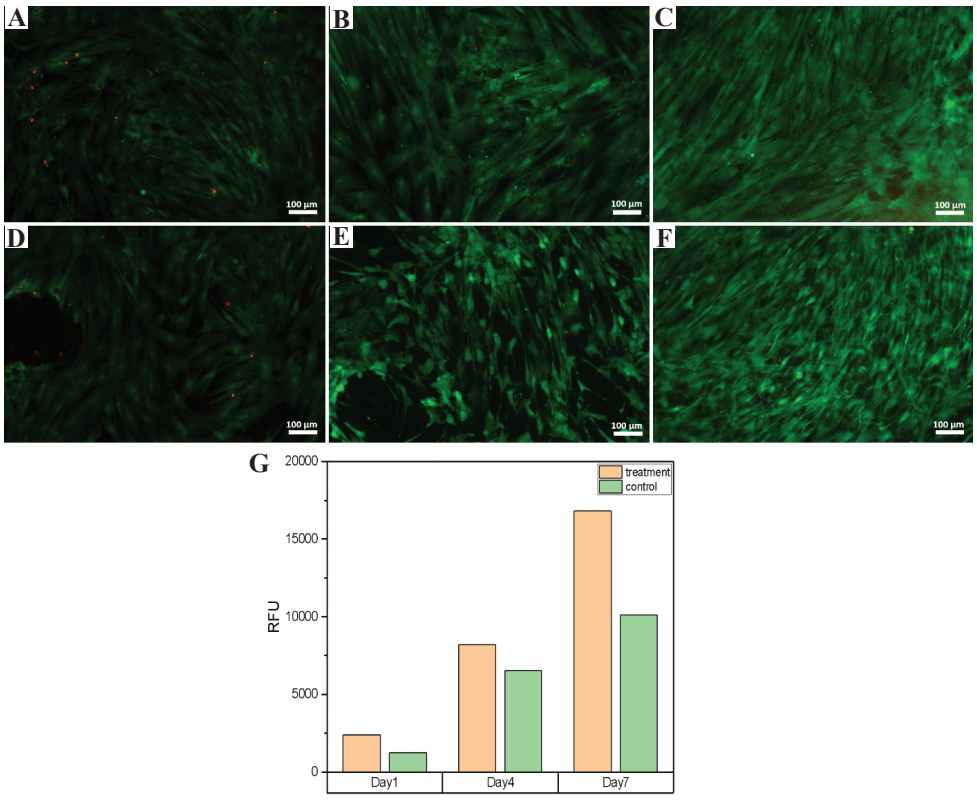

Figure 7. Biological assessments. Growth of MSCs cultured in direct contact with the developed ink during (A) 1, (B) 4, and (C) 7 days. The cells were also cultured in 2D for the same amount of time; (D), (E), and (F) served as the control. (G) Amount of metabolically active MSCs during 1, 4, and 7 days. These cells were cultured with the ink (treatment) and with growth media (control). The assay was quantified in terms of relative fluorescence units (RFU).

of the components. The final loss from the 39% of the material comes from the calcium carbonate in the sample; the rest comes from some residues from hydroxyapatite; which is the strongest component to decompose by heat in this formulation[23]. In the DSC (**Figure 5B**), as several distinct chemical behaviors are coming from different sources of crosslinking and the inorganic composition, the initial broad peak corroborates the TGA statement of dehydration. Furthermore, it can be stated that a glass transition (Tg) can be observed in the shoulder at 175°C, a slight crystallization point (Tc) can be observed at the exothermic downslide at 225°C, and finally a melting point (Tm), presumably all organic compounds coming from biopolymers, can be detected at 260°C in the endothermic peak[30].The viscoelastic properties of the ink were determined using an oscillatory rheology test. The mechanical stiffness of the non-crosslinked ink was found to be 5.80 kPa, which was assessed from the average of storage modulus (G') in 5 min measurement (**Figure 6A**). The ink with a higher G' value compared to the loss modulus (G'') usually provides good shape fidelity for the printed construct[18]. The thermal stability of the ink was also investigated using a temperature-dependent rheological test (**Figure 6B**). The result suggests that the stiffness of the ink can be tuned by increasing the temperature. The viscosity of the ink during the extrusion was found to be 117 Pa·s, which was determined from the calculated shear rate of the nozzle of 8.60 s^{-1} (**Figure 6C**).

The biological assessment results in **Figure 7A-F** show the biocompatibility of the developed ink with biological organisms, such as the MSCs. It was observed that during the initial 4 days of interaction with the developed ink, an accelerated growth was achieved by the MSCs when cultured in the presence of the ink, in comparison to when only being cultured in media. Moreover, after 7 days (**Figure 7G**), the amount of metabolically active cells was higher in the presence of the ink in comparison to using media. These findings demonstrate the excellent biocompatibility of the developed ink with biological entities and highlight the potential of this ink to be used in tissue engineering applications.

4. Conclusions

This project expanded the frontiers of biomaterials commonly used in regenerative medicine to assist in finding the solution for the latent problem in the marine environmental ecosystem – coral bleaching. Therefore, we developed an eco-friendly ink that can potentially be used to restore rigid living systems. Based on a wide range of previous investigations in biomaterials applied for bone and cartilage tissue regeneration, our ink is composed of biopolymers as gelatin, alginate, GelMA, and PEGDA with the integration of bioceramics as calcium carbonate and hydroxyapatite, which are fundamental for mimicking the structures of corals. We demonstrated the effectiveness of the ink to be manufactured by 3D molding and printing technologies, which is a crucial step to develop complex figures that could mimic a coral and serve as a scaffold for biological systems as polyps. Furthermore, we implemented an image processing and surface analysis to find a more accurate concentration of ceramics imbued in the biopolymers. This innovative analysis provides a new opportunity to mitigate the lack of characterization methods to improve the printability fidelity of novel bioinks. The photo-crosslinking behavior coming from GelMA, PEGDA, and ionic-crosslinking of alginate make the ink stable for complex physicochemical conditions, as the seawater ecosystem, in which there is an excess of cations are coming from calcium sources. This presents a possibility for *in situ* appliances in coral reefs with the aid of diverse 3D manufacturing technologies, as shown in the schematic overview in **Figure S7**.

Furthermore, the chemical characterization corroborates the interaction of the materials and the crosslinking behavior seen at the infrared spectra peaks for ionic-crosslinking at 3300 cm^{-1} and photo-crosslinking at 2950-90 cm^{-1}. In addition, X-Ray diffraction clearly shows the convergence of calcium carbonate and hydroxyapatite without altering its ground state crystal structure, corroborating that no other chemical or physical methods are needed for its preparation. Using this method, the product can be easily produce in a cost-effective manner. Moreover, NMR corroborates the interaction of calcium, phosphate, and carbonate ions from the bioceramics in the biopolymer matrix. Besides, thermochemical characterization with TGA and DSC gives us an initial insight into how the material works with the temperature appliance, which works perfectly for our final scope. In addition, discussion related to the mechanical properties of the ink, with different tests of rheology to evaluate storage/loss modulus in terms of time and temperature, and its viscosity versus shear rate, corroborates the potential printability of the precrosslinked ink for manufacturing complex structures. Finally, a biological assessment was done with MSCs to demonstrate the material's biocompatibility with living MSCs; we suggest that the material could potentially be used for different living systems. In conclusion, the material can withstand harsh conditions, and the degradation rate can be controlled with the specific behavior from each constituent of the ink. This formulation is the beginning of future investigations as it has potential use for rigid living systems with interesting tunable properties that could fulfill different directions regarding the final user's needs.

Acknowledgments

Team members of the group developed graphical abstract and technical assistance from the biotech artist Alma R.

García-Roche. In addition, supplementary figures were designed and created with the aid of http://biorender.com/. This work was financially supported by the King Abdullah University of Science and Technology.

Conflicts of interest

The authors declare that they do not have any competing interests.

Authors' Contributions

C.A.E.H. guided and supervised the project. A. A. R. designed and supervised the experiments. A. A. R., A.U.V.P., H.H.S., G.B., R.P.P., A. A., and Z. K. conducted experiments and contributed intellectually to the scientific design of the project. P.B. mentored the technical part of the project.

References

1. Chesterman J, Zhang Z, Ortiz O, *et al*., 2020, Biodegradable Polymers. In: Principles of Tissue Engineering. 5th ed., Ch. 18. Academic Press, United States, p317-342. https://doi.org/10.1016/j.matpr.2020.01.437
2. Biswal T, BadJena SK, Pradhan D, 2020, Sustainable Biomaterials and their Applications: A Short Review. *Mater Today*, 30:274–82.
3. Simionescu BC, Ivanov D, 2015, Natural and Synthetic Polymers for Designing Composite Materials. In: Handbook of Bioceramics and Biocomposites. Ch. 11-1. Wiley-VCH: Weinheim, Germany, p1–54. https://doi.org/10.1007/978-3-319-09230-0_11-1
4. Lee M, Rizzo R, Surman F, Zenobi-Wong M, 2020, Guiding Lights: Tissue Bioprinting Using Photoactivated Materials. *Chem Rev*, 120:10950–1027. https://doi.org/10.1021/acs.chemrev.0c00077
5. Chimene D, Miller L, Cross LM, *et al*., 2020, Nanoengineered Osteoinductive Bioink for 3D Bioprinting Bone Tissue. *ACS Appl Mater Interfaces*, 12:15976–88. https://doi.org/10.1021/acsami.9b19037
6. Zhou H, Lee J, 2011, Nanoscale Hydroxyapatite Particles for Bone Tissue Engineering. *Acta Biomater*, 7:2769–81.
7. Kelly BE, Bhattacharya I, Heidari H, *et al*, 2019, Volumetric Additive Manufacturing Via Tomographic Reconstruction. *Science*, 363:1075–9. https://doi.org/10.1126/science.aau7114
8. Leggat WP, Camp EF, Suggett DJ, *et al.*, 2019, Rapid Coral Decay is Associated with Marine Heatwave Mortality Events on Reefs. *Curr Biol*, 29:2723–30.e4. https://doi.org/10.1016/j.cub.2019.06.077
9. Mass T, *et al.*, 2017, Amorphous Calcium Carbonate Particles form Coral Skeletons. *Proc Natl Acad Sci*, 114:E7670–8. https://doi.org/10.1073/pnas.1707890114
10. Wangpraseurt D, You S, Azam F, *et al.*, 2020, Bionic 3D Printed Corals. *Nat Commun*, 11:1748.
11. Yu AC, Reinhart M, Hunter R, *et al.*, 2021, Seasonal Impact of Phosphate-Based Fire Retardants on Soil Chemistry Following the Prophylactic Treatment of Vegetation. *Environ Sci Technol*, 55:2316–23. https://doi.org/10.1021/acs.est.0c05472.s001
12. Loessner D, Meinert C, Kaemmerer E, *et al.*, Functionalization, Preparation and use of Cell-laden Gelatin Methacryloyl-based Hydrogels as Modular Tissue Culture Platforms. *Nat Protoc*, 11:727–46. https://doi.org/10.1038/nprot.2016.037
13. Khan Z, Kahin K, Rauf S, *et al.*, 2019, Optimization of a 3D Bioprinting Process Using Ultrashort Peptide Bioinks. *Int J Bioprint*, 5:173. https://doi.org/10.18063/ijb.v5i1.173
14. Gong J, Schuurmans CC, van Genderen AM, *et al.*, 2020, Complexation-induced Resolution Enhancement of 3D-Printed Hydrogel Constructs. *Nat Commun*, 11:1267.
15. Gonzalez-Rios JA, Valle-Pérez AU, Amaya-Delgado L, *et al*., 2021, A Quick Fed-batch Saccharification Strategy of Wheat Straw at High Solid Loadings Improving Lignocellulosic Ethanol Productivity. *Biomass Conversion Biorefinery*. https://doi.org/10.1007/s13399-021-01580-0
16. Valle-Pérez AU, Flores-Cosío G, Amaya-Delgado L, 2021, Bioconversion of Agave Bagasse to Produce Cellulases and Xylanases by *Penicillium citrinum* and *Aspergillus fumigatus* in Solid-State Fermentation. *Waste Biomass Valorization*. https://doi.org/10.1007/s12649-021-01397-y
17. Susapto HH, Alhattab D, Abdelrahman S, *et al.*, 2021, Ultrashort Peptide Bioinks Support Automated Printing of Large-Scale Constructs Assuring Long-Term Survival of Printed Tissue Constructs. *Nano Lett*, 21:2719–29. https://doi.org/10.1021/acs.nanolett.0c04426.s010
18. Theus AS, Ning L, Hwang B, *et al.*, 2020, Bioprintability: Physiomechanical and Biological Requirements of Materials for 3D Bioprinting Processes. *Polymers* (*Basel*), 12:2262. https://doi.org/10.3390/polym12102262
19. Doostmohammadi A, Monshi A, Salehi R, *et al.*, 2011, Cytotoxicity Evaluation of 63s Bioactive Glass and Bone-Derived Hydroxyapatite Particles Using Human Bone-marrow Stem Cells. *Biomed Pap Med Fac Univ Palacky Olomouc Czech Repub*, 155:323–6. https://doi.org/10.5507/bp.2011.028

20. Parvez S, Rahman MM, Khan MA, *et al.*, 2012, Preparation and Characterization of Artificial Skin Using Chitosan and Gelatin Composites for Potential Biomedical Application. *Polym Bull*, 69:715–31. https://doi.org/10.1007/s00289-012-0761-7
21. Guo X, Liu L, Wang W, *et al*., 2011, Controlled Crystallization of Hierarchical and Porous Calcium Carbonate Crystals Using Polypeptide Type Block Copolymer as Crystal Growth Modifier in a Mixed Solution. *Cryst Eng Commun*, 13:2011. https://doi.org/10.1039/c0ce00202j
22. Saarai A, Kasparkova V, Sedlacek T, *et al*., 2013, On the Development and Characterisation of Crosslinked Sodium Alginate/Gelatine Hydrogels. *J Mech Behav Biomed Mater*, 18:152–66. https://doi.org/10.1016/j.jmbbm.2012.11.010
23. Aldana AA, Malatto L, Rehman MA, *et al*., 2019, Fabrication of Gelatin Methacrylate (GelMA) Scaffolds with Nano- and Micro-Topographical and Morphological Features. *Nanomaterials*, 9:120. https://doi.org/10.3390/nano9010120
24. Kontoyannis CG, Vagenas NV, 2000, Calcium Carbonate Phase Analysis Using XRD and FT-Raman Spectroscopy. *Analyst*, 125:251–5. https://doi.org/10.1039/a908609i
25. Manafi SA, Yazdani B, Rahimiopour MR, *et al*., 2008, Synthesis of Nano-hydroxyapatite under a Sonochemical/ Hydrothermal Condition. *Biomed Mater*, 3:025002. https://doi.org/10.1088/1748-6041/3/2/025002
26. Duan P, Li X, Wang T, *et al.*, 2018, The Chemical Structure of Carbon Nanothreads Analyzed by Advanced Solid-State NMR. *J Am Chem Soc*, 140:7658–66. https://doi.org/10.1021/jacs.8b03733
27. Zhu M, Wang Y, Ferracci G, *et al*., 2019, Gelatin Methacryloyl and its Hydrogels with an Exceptional Degree of Controllability and Batch-to-Batch Consistency. *Sci Rep*, 9:6863. https://doi.org/10.1038/s41598-019-42186-x
28. Raveendran NT, Vaquette C, Meinert C, *et al*., 2019, Optimization of 3D Bioprinting of Periodontal Ligament Cells. *Dent Mater*, 35:1683–94. https://doi.org/10.1016/j.dental.2019.08.114
29. Tan F, Xu X, Deng T, *et al*., 2012, Fabrication of Positively Charged Poly(Ethylene Glycol)-Diacrylate Hydrogel as a Bone Tissue Engineering Scaffold. *Biomed. Mater*, 7:055009. https://doi.org/10.1088/1748-6041/7/5/055009
30. Gill P, Moghadam TT, Ranjbar B, 2010, Differential Scanning Calorimetry Techniques: Applications in Biology and Nanoscience. *J. Biomol. Technol*., 21:167–193.